Journal of Alloys and Compounds xxx (2012) xxx–xxx

Contents lists available at SciVerse ScienceDirect

Journal of Alloys and Compounds

journal homepage: www.elsevier.com/locate/jallcom

Characteristics of Japanese sword produced from *tatara* steel

Chihiro Matsumoto, Ananda Kumar Das, Takuya Ohba*, Shigekazu Morito, Taisuke Hayashi, Go Takami

Shimane University, Department of Materials Science, Nishikawatsu-1060 Matsue, Shimane 690-8504, Japan

ARTICLE INFO

Article history:
Available online xxx

Keywords:
Japanese sword
Steel
Lath martensite
Tatara

ABSTRACT

Japanese sword are understood that they contain martensite and could not be produced without *tamahagane* steel by *tatara* process. A newly produced sword (short sword) prepared from *tamahagane* steel using traditional forge-folding (*tatara*) method was examined by optical microscopy and SEM/EBSD method for observing the microstructural features in it. It was found that the microstructure of the sword was martensite with lath type morphology. The feature of lath martensite was characterized by observing the prior austenite grain, packet and block boundaries with respect to their linearity and curviness. Thus a new method of comparison between *tatara* steel and ordinary Fe–C steel was mentioned by measuring the curved line and the straight line contained in the boundaries corresponding to the prior austenite grains, packets and blocks.

1. Introduction

Tatara is a traditional process of making steel developed in Japan. The steel is called *tamahagane* and are manufactured with iron sand smelted by charcoal in a special type of furnace (smelter) made from sand and clay. The *tamahagane* is utilized for producing Japanese sword, which is tough and strong enough. It is said that Japanese sword cannot be produced without *tamahagane* [1]. In our previous study [2,3], we found a lot of inclusions in a new Japanese sword (short sword) prepared by a famous swordsmith using tamahagane and compared its features with those of ordinary Fe–C steel. Yaso et al. studied an old Japanese sword and described that it also contained a lot of inclusions [4]. In general, the inclusions are thought to be origins of cracks in the metallic object but no cracks were found in the Japanese swords, although they are contained. The quality of toughness and strength is achieved by its microstructure as a functionally graded material; that is, ferrites are distributed inside and martensites are distributed outside on the surface of the sword. The characteristic of martensite on the surface is lath martensite [2], which is achieved by a special quenching process after successive forge-folding operations. The forge-folding process has an impact on controlling the carbon content [5,6] as well as to refine grain size in the matrix. Carbon content affects the microstructure and causes the hardness of the steel. Lath martensite is reported to appear in the steel containing the carbon less than 0.8 mass% [6].

Lath martensite is characterized by blocks and packets in a prior austenite grain. Mechanical property of lath martensite is deeply related to the sizes of block and packet [4–8]. So the aim of this study is to compare the block, packet and the prior austenite grain to those of the Fe–C ordinary steels. Those boundaries are constructed to be straight lines and curved lines under some magnifications. The curved boundaries have different curvature at place to place. Thus the features of the block, packet and prior austenite grain boundaries are described in a new manner for comparing the short sword made from *tamahagane* and in ordinary Fe–C steel.

2. Experimental procedures

Three kinds of specimens were employed in this study. The first one is short sword prepared by a famous Japanese swordsmith using a traditional (*tatara*) method. The short sword is (approx. size: 180 mm × 12 mm × 4 mm) shown in Fig. 1(a), and cross section of the short sword is shown in Fig. 1(b). The short sword was cut into pieces using a computer controlled spark wire cutter. The observations of the microstructure have been performed on the cross-section. The chemical analysis of short sword was performed. The second and third specimens are ordinary Fe–C steel specimens having the chemical composition Fe–0.61C–0.014Si–0.01Mn–0.003P–0.005S (mass%), and Fe–0.78C–0.03Si–0.03Mn–0.005P–0.005S (mass%). Both of the specimens were annealed at 1073 K for 0.6 ks and then quenched into water. They are abbreviated to be 0.6 and 0.8 mass%C hereafter. The observations by optical microscopy (OM), scanning electron microscopy (SEM, JEOL JSM-7001FA) with electron back-scatter diffraction (EBSD) were carried out for examining the morphologies. Further, EPMA measurements of the short sword were performed using a JXA 8800 M electron probe micro analyzer.

3. Results and discussion

3.1. EPMA observations

The result of the chemical analysis is shown in Table. 1. EPMA measurements indicated that the carbon content is not uniform and varies from 0.6 to 2.0 mass%C in the sharp end. At the sharp

* Corresponding author.
E-mail addresses: s119133@matsu.shimane-u.ac.jp (C. Matsumoto), ohba@riko.shimane-u.ac.jp (T. Ohba), mosh@riko.shimane-u.ac.jp (S. Morito).

0925-8388/$ – see front matter © 2012 Elsevier B.V. All rights reserved.
http://dx.doi.org/10.1016/j.jallcom.2012.05.039

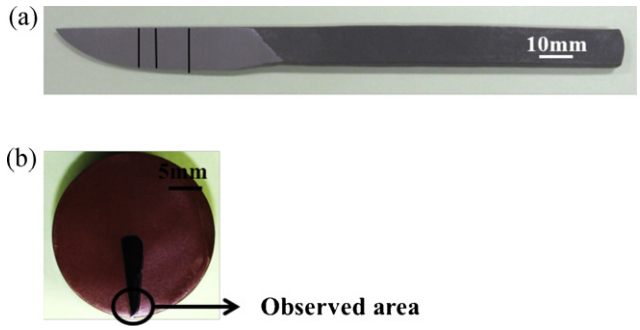

Fig. 1. (a) Photograph of the short sword employed in present study, (b) photograph of cross section view of the short sword which cut piece for observation.

Table 1
Chemical analysis in the short sword (mass%).

C	Na	Mg	Si	Ti	Mn	Al	K	Ca	Fe
0.624	0.007	0.0005	0.01	0.004	0.004	0.003	0.01	0.001	Bal.

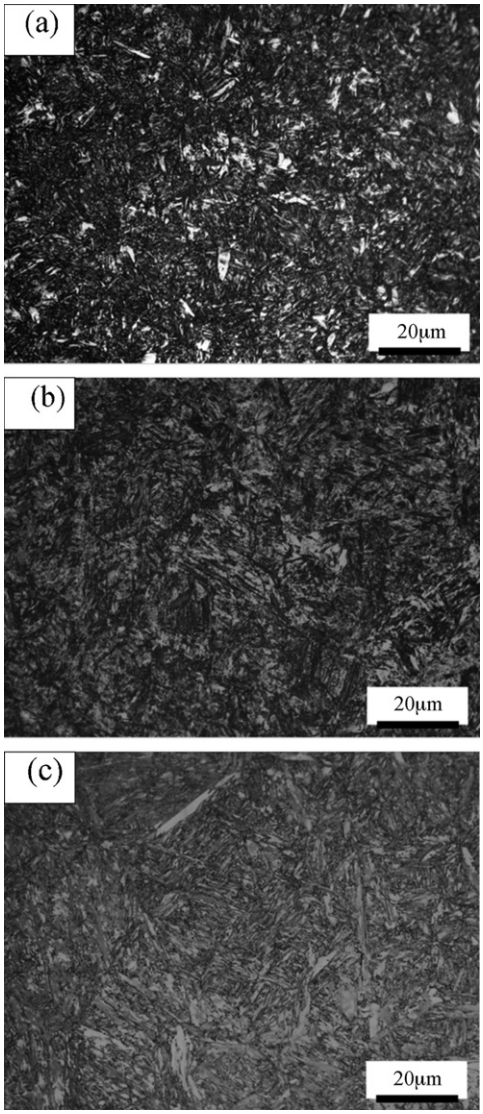

Fig. 2. Optical micrographs: (a) cross section of the short sword (b) and (c) Fe–0.6 and Fe–0.8 mass% C respectively.

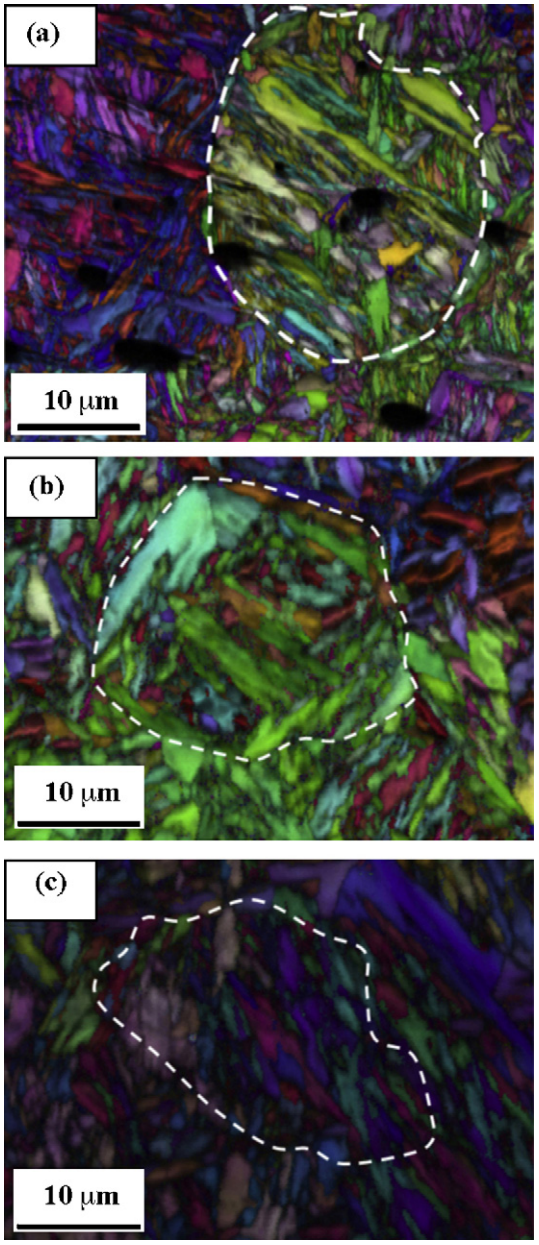

Fig. 3. Crystal orientation maps: (a) cross section of the short sword (b) and (c) Fe–0.6 and Fe–0.8 mass%C respectively. The white dotted line showed one austenite grain.

Table 2
The result of the martensitic structure size measurement using SEM/EBSD.

	Cross section of the short sword	0.6 mass%C steel	0.8 mass%C steel
Block thickness	0.47 μm	0.57 μm	0.65 μm
Packet size	3.6 μm	5.3 μm	6.7 μm
Prior austenite grain size	20 μm	18 μm	20 μm
Straight line portion	0.73	–	0.35

end along the short sword, the carbon content was lower compared with the ridge end, which is other side of sharp end. The morphology measurements were performed around the sharp end. The carbon content around the analyzed area was about 0.73 mass%.

Please cite this article in press as: C. Matsumoto, et al., J. Alloys Compd. (2012), http://dx.doi.org/10.1016/j.jallcom.2012.05.039

Table 3
The SEM/EBSD conditions at the time of the measurement.

Criteria of EBSD images
Scanning step size: 1 μm
Scanning area = 100 × 100 μm
Magnification: × 500
Working distance: 15 mm
Voltage: 25 kV

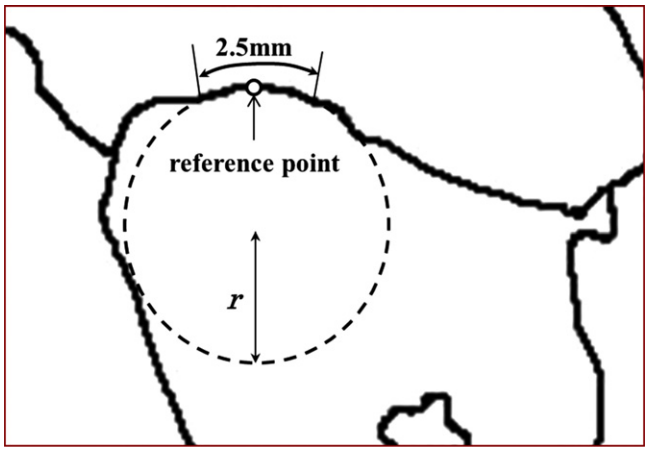

Fig. 4. How to calculate curvature. The solid line is the packet grain boundary. The white dot is the reference point 0.25 μm in diameter. The segment of 2.5 μm in length from the neighbor of the reference point is fitted to the circle of the radius *r*.

3.2. Optical microscopy and SEM/EBSD observations

Fig. 2(a) shows the OM image of cross section of short sword. Fig. 2(b) and (c) show the OM images of ordinary Fe–C steel for 0.6 and 0.8 mass%C, respectively. They showed the lath martensite morphology.

Fig. 3 shows the crystal orientation maps obtained by SEM/EBSD measurements. The white dotted lines in Fig. 3 shows the austenite grain boundary. Fig. 3(a) shows the crystal orientation map taken from the short sword. The austenite grain boundary is not clear, and the packets as well as the blocks boundaries are irrationally arranged. The average block thickness has been found to be 0.47 μm and the average packet size is 3.6 μm. A similar measurements were performed for the ordinary Fe–C steel to compare the morphology with the short sword. Fig. 3(b) and (c) show the crystal orientation maps of these specimens. The average block thickness is 0.57 and 0.65 μm in 0.6 and 0.8 mass%C, respectively. The average packet sizes are found to be 5.3 and 6.7 μm in 0.6 and 0.8 mass%C Fe–C ordinary steel, respectively. It was found that the size of block and packet is comparatively smaller in the short sword. Table 2 showed the result of the martensitic structure size measurement using SEM/EBSD.

To make the characteristics of the martensite clearer, the following two kinds of analysis were performed. (1) Measurements of curvature in the packet boundaries of lath-martensite and (2) measurements of length of straight-line portion in prior austenite grain boundaries for both of the short sword and ordinary Fe–C steel. The data analysis were performed with using SEM/EBSD images with OIM analysis – software version 5.2 of TSL–EDAX Ltd. The conditions for the measurements are listed in Table 3. EPMA measurements indicated that carbon content of short sword is not

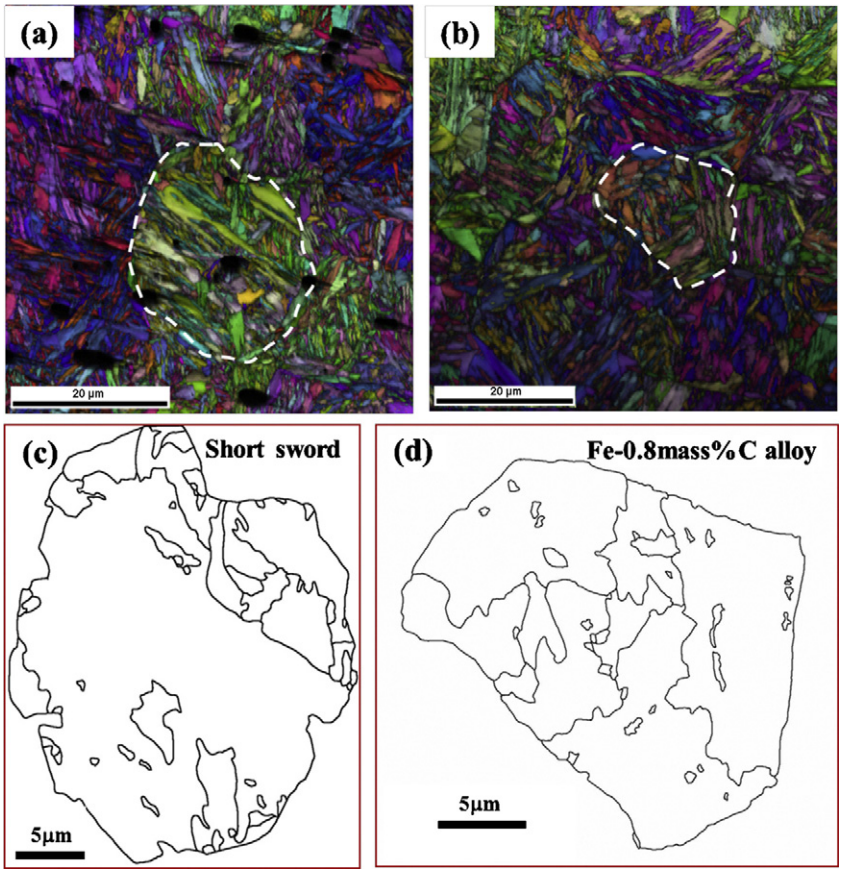

Fig. 5. Crystal orientation maps and distribution of packets in the austenite grain: (a) and (c) cross section of the short sword, (b) and (d) Fe–0.8 mass%C. The lines which segment the inside of grain into small groups were the packet boundaries.

Please cite this article in press as: C. Matsumoto, et al., J. Alloys Compd. (2012), http://dx.doi.org/10.1016/j.jallcom.2012.05.039

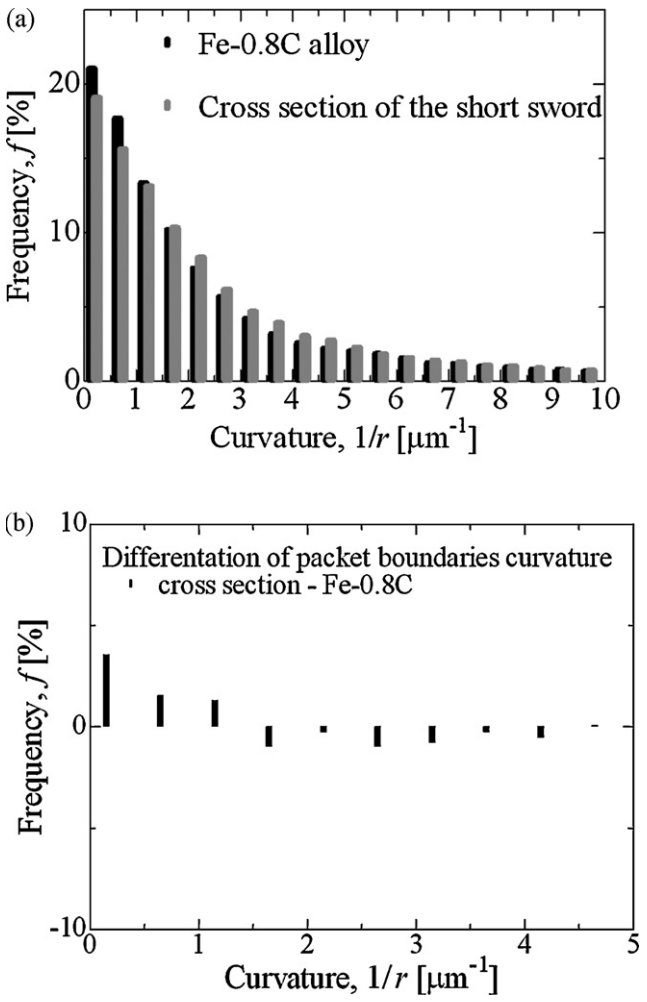

Fig. 6. (a) Curvature distribution of packet boundary in short sword and Fe–0.8 mass%C, (b) difference of curvature distribution of packet boundary in short sword and Fe–0.8 mass%C.

uniform. Although the carbon content changes gradually at the transitional region from inside ferrite to outside martensite, the carbon content around the sharp end is almost uniform.

3.3. Curvature measurements in packet boundary of martensite

Curvature at every point on the packet grain-boundary was measured for short sword and 0.8 mass%C steel. A schematic view of the curvature measurements was shown in Fig. 4. We selected the reference point at every 0.25 μm along the packet boundaries, and the segment of 2.5 μmin length from the neighbor of the reference point was fitted to the circle of the radius r. We defined that the curvature was $1/r$ (μm^{-1}).Fig. 5(a) and (b) show the crystal orientation maps for short sword and 0.8 mass%C, respectively. The white dotted lines indicate prior austenite grain boundaries. Fig. 5 (c) and (d) show the tracies of the packet boundaries of each specimens.

Using above figures, histogram was drawn for short sword and 0.8 mass%C steel and shown in Fig. 6 (a).The black bar shows the frequency of 0.8 mass%C steel and the gray bar shows the frequency of the short sword. The frequency of the short sword is lower at small curvature. To make difference clearer, the difference between 0.8 mass%C and short sword, corresponding to black and gray, was taken up to 3 $\mu m^{-1}$and shown in Fig. 6(b). As indicated above, differences are found at smaller curvatures. The smaller curvature is long wavelength wavy pattern and larger curvature is short wavelength wavy pattern. The frequency of smaller curvature of the 0.8 mass%C steel is higher than that of the short sword. This means that boundaries in short sword consist of short wavelength wavy patterns, smaller zig-zag patterns, compared with 0.8 mass%C steel.

3.4. Measurements of length of straight-line portion of lath-martensite

As indicated above, boundaries of the short sword looks smaller zig-zag pattern compared with those of 0.8 mass%C steel. The smallest limit of curvature is straight line. When the prior austenite grain boundaries were observed, the boundaries look straight. Thus the following value were calculated for getting prior austenite grain boundary characteristics. In this measurement, one typical prior austenite grain was chosen for getting values of equation shown in Fig. 7. The ratio of straight line length to total peripheral line length, ξ, was calculated and schematic figure is shown in Fig. 7. The austenite grain boundaries used for straight line portion measurements were shown in Fig. 8. The definition of straight line is difficult, because straight line may change under larger magnification. In this study, we defined a straight line as 5 μm length or more by eyes under the magnification of 500 with optical microscope. The results of ξ value for 0.8 mass%C steel is 0.73 and that for short sword is 0.35. This tendency is consistent with curvature measurements, although curvature measurements were performed on packet boundaries and straight line measurements were performed on prior austenite boundaries.

The boundary of martensite and prior austenite grain was characterized by straight line measurements and curvature measurements. The boundaries of the short sword showed lower frequency at small curvature indicating smaller zig-zag pattern and low ξ indicating shorter straight line portion. On the other hand, boundaries on 0.8 mass%C steel showed higher at small curvature and high ξ value. These parameters may be related to the mechanical property on Japanese sword evidently. Further research on boundary characteristics is necessary for clarifying the relationship between the mechanical property and the microstructure of martensite.

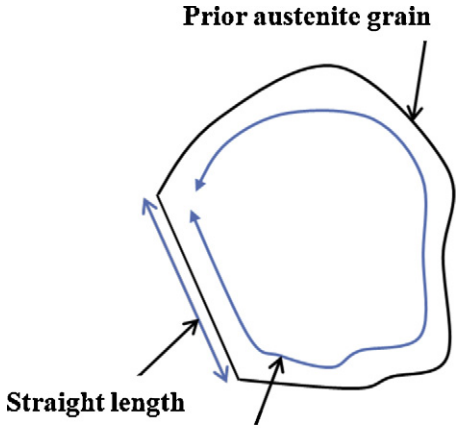

$$\xi = \frac{Straight\ length}{Total\ peripheral\ length}$$

Fig. 7. View showing a frame format of measurement part of straight line portion and definitional identity of straight line portion.

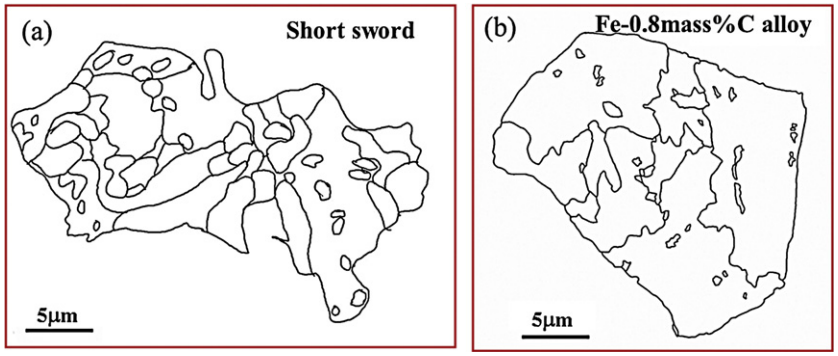

Fig. 8. The figures of the austenite grain boundary used for straight line measurements. An outside line of the austenite grain boundary is used for measurement.

Previous study [9] showed that the short sword contained many inclusions. They are fayalite (Fe_2SiO_4), cementite and SiO_2 etc., and are distributed over the whole part of the short sword. Vedantam et al. discussed the interaction of grain boundaries and particles (supposed to be inclusions in this paper) with phase field method; that is, inclusions affect grain growth rate and pinning effect on polycrystalline [10]. They mentioned that the boundary away from the particle continues to evolve, increasing the curvature near the particle. Thus the distribution of particles affect the curvature; *i.e.*, the grain boundaries having large curvature distributed near the particles. Their result that distribution of inclusions affect the curvature may be also on the short sword. Actually, the short sword, which contained a lot of inclusions, has low frequency at small curvature compared with 0.8 mass%C steel. Inclusions were related to the feature of the morphology of martensite which studied here. In our further study, we will discuss the influence of inclusions on morphology and formation of microstructure in detail.

4. Conclusion

The short sword prepared from *tamahagane* by traditional technique was observed by optical microscopy and SEM/EBSD measurements. The sizes of lath martensite were identified with average block thickness 0.47 μm and packet size 3.6 μm, respectively, which were smaller than those of Fe–C steel. The morphology of packet and prior austenite grain boundaries were quantified, and it was found that the boundaries in the short sword has small curvature and small ratio of straight line compared with ordinary Fe–C steel. It was understood by this analysis that grain boundary of the short sword is short wavelength wavy patterns.

Acknowledgements

The authors are greatly indebted to Mr. Sadanao Mikami, a famous Japanese swordsmith for providing the sword for present study. We are grateful to Dr. Onda, Department of Mechanical Engineering, Tottori University, for help in EPMA measurements. We also acknowledge Mr. Ichinotani, who graduated from the graduate school of Shimane University, for his help in SEM/EBSD data analysis.

References

[1] Leon, Hiroko Kapp, Yoshindo Oshihara: The Craft of the Japanese Sword, Kodansha International Ltd., Tokyo Japan, 1987, First edition, pp. 30.
[2] A. K. Das, T. Ohba, S. Morito, G. Takami, T. Fujikawa, M. Yaso. http://dx.doi.org/10.1051/esomat/200902024.
[3] A.K. Das, T. Ohba, S. Morito, M. Yaso, Materials Science Forum 654–656 (2010) 138–141.
[4] M. Yaso, T. Takaiwa, Y. Minagi, K. Kubota, S. Morito, T. Ohba, A. K. Das. http://dx.doi.org/10.1051/esomat/200907018.
[5] N. Sasaki, T. Horii, M. Fujiwara, H. Saitoh, T. Misawa, Tetsu-to-Hagane 86 (2000) 45–50.
[6] N. Sasaki, T. Momono, Tetsu-to-Hagane 93 (2007) 78–84.
[7] Hiromoto Kitahara, Rintaro Ueji, Nobuhiro Tsuji, Yoritoshi Minamino, Acta Materialia 54 (2006) 1279–1288.
[8] G. Krauss, Materials Science and Engineering A273–275 (1999) 40–57.
[9] G. Takami, T. Ohba, S. Morito, A.K. Das, Materials Science Forum 654–656 (2010) 134–137.
[10] S. Vedantam, A. Mallick, Acta Materialia 58 (2010) 272–281.